Supporting information

Examining Interfacial Kinetics on Electrostatically Heterogeneous Surfaces using ζ-potential measurements

Ramya Kumar,[†,‡] Irina Kopyeva,[†,‡] Kenneth Cheng,[¶,‡] Kai Liu,[†] and Joerg Lahann[*,†,‡,§,¶,‖]

†*Department of Chemical Engineering, University of Michigan, Ann Arbor*

‡*Biointerfaces Institute, University of Michigan, Ann Arbor*

¶*Department of Material Science & Engineering, University of Michigan, Ann Arbor*

§*Department of Macromolecular Science & Engineering, University of Michigan, Ann Arbor*

‖*Department of Biomedical Engineering, University of Michigan, Ann Arbor*

E-mail: lahann@umich.edu

Phone: +173 4763 7543

1 Fourier Transform Infrared Spectroscopy

For the the SI-ATRP initiator coating, poly[(p-xylylene-4-methyl-2-bromoisobutyrate)-co-(p-xylylene)] (PPX-EB), the FTIR spectrum is shown in Fig S1A. Peaks at 1730 cm^{-1} (carbonyl stretch) and 1160 cm^{-1} (C-O-C stretches of the ester group) were used to ascertain that initiator groups were present.

For the poly(4-ethynyl-p-xylylene-co-p-xylylene) (PPX-alkyne) coating (Fig S1B), the presence of reactive alkyne groups was visible in the 3286 cm^{-1} peak representing the alkyne C-H stretch and in the signal at 2100 cm^{-1}, which can be attributed to the carbon-carbon triple bond.

A) B)

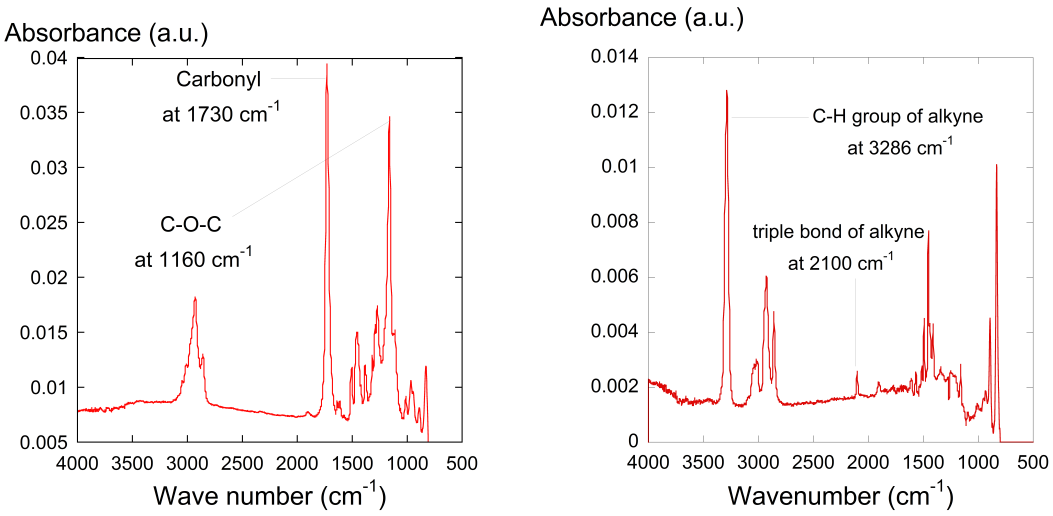

Figure S1. A)IRRAS spectrum of the PPX-EB ATRP initiator coating prepared using CVD. B)IRRAS spectrum of PPX-alkyne

The copolymer, poly[(p-xylylene-4-methyl-2- bromoisobutyrate)-co- (p-xylylene- 4-aminomethyl)-co-(p- xylylene) was composed of ester bromide and aminomethyl functional groups. FTIR spectra were used to assess the ratio of the two functional groups (Fig S2A). The intensities of the carbonyl stretch at 1730 cm^{-1} and the C-O- C peaks at 1160 cm^{-1} relative to the intensity of the N-H stretch of the aminomethyl groups, located at 3300 cm^{-1} was observed to vary with copolymer composition.

To confirm the successful synthesis of the sorbitol methacrylate brush, the hydroxyl group was used. This has a distinctive broad peak in the region of 3300-3400 cm^{-1} and is the only peak unique to the glycopolymer. After the SI-ATRP of sorbitol methacrylate, the signal from the hydroxyl moiety overlapped with the N-H peak, leading to a higher peak intensity in this wavenumber region. Similarly, the carbonyl of the sorbitol brush (1730 cm^{-1}) and the C-O peaks of the sorbitol side chain (1160 cm^{-1}) served to amplify pre-existing peaks in these wavenumbers from the ester bromide from the initiator groups. (Fig S2B).

A) B)

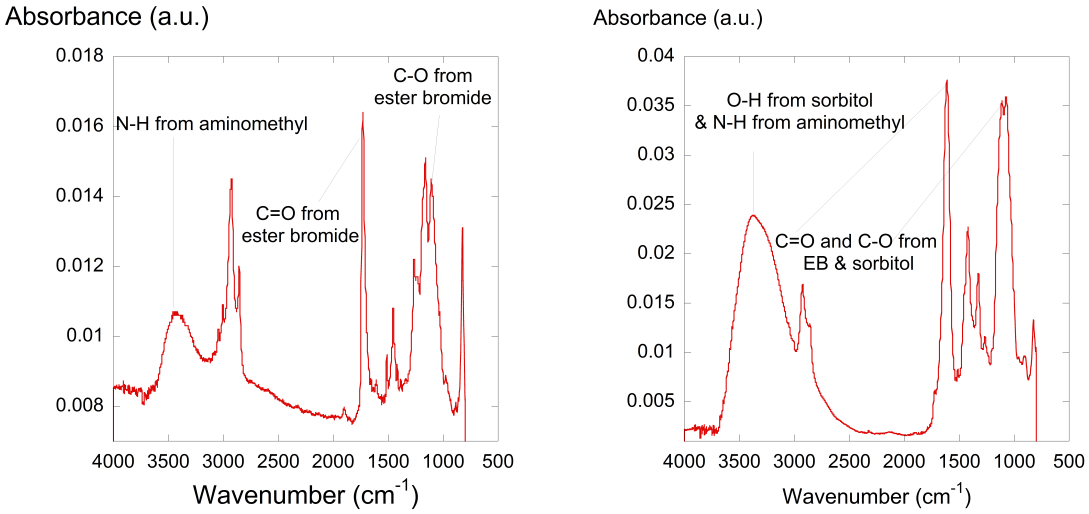

Figure S2. A)IRRAS spectrum of the copolymer consisting of the SI-ATRP initiator (ester bromide) and binding site (aminomethyl) groups prepared using CVD copolymerization. B)IRRAS spectrum of sorbitol methacrylate when polymerized from the copolymer.

2 Ellipsometric measurements

We observed that the values of the brush thickness tended to increase with increasing ester bromide surface concentrations. A higher initiator density is likely to improve grafting density, resulting in thicker brushes. The results are summarized in Table S1

Table S1. Thickness of sorbitol brush measured from copolymers of different compositions

Copolymer	Thickness in nm from two experimental runs	
Copolymer with IEP 3.6	8.1	9.3
Copolymer from Fig 4.8	6.7	7.7
Copolymer from Fig 5.7	4.5	1.5

3 Kinetic modeling results

Experimental data obtained from the electrokinetic analyser and QCM values were fitted according to the following equation.

$$y = A(1 - e^{-kt})$$

The apparent rate constants (k) and adsorption plateau values (A) were extracted using MATLAB's curve fitting module. The extracted model parameters for real-time ζ-potential measurement and QCM are tabulated in Table S2 and Table S3 respectively. Plots comparing experimental data with the model trajectory are shown in Figure S3 and Figure S4. In general the model values were in agreement with the experimental values. In the case of the ζ-potential measurement performed at 1000 nM neutravidin, outliers had to be removed manually to obtain a better fit. Model diagnostic tests reveal that the model was successful in capturing experimental trends as seen in Table S4 and Table S5.

Table S2. Summary of fitting results for real-time ζ-potential measurements of neutravidin-biotin binding. As expected, the rate constant and adsorption plateau were observed to increase with increasing neutravidin concentration.

Neutravidin Concentration	k *10^3 (sec-1)	A (mV)
10 nM	4.164$\pm$0.094	19.14$\pm$0.09
100 nM	7.96$\pm$0.184	23.37$\pm$0.08
1000 nM	29.88$\pm$0.07	29.88$\pm$0.07

Table S3. Summary of fitting results for QCM measurements of neutravidin-biotin binding. Like the ζ-potential measurements, a monotonic increase of adsorption response with neutravidin concentration was observed. However, the value of the apparent rate constant for the 10 nM experiment seems too high, possibly due to transient fluctuations in the flow.

Neutravidin Concentration	k *10^3 (sec-1)	A (ngcm-2)
10 nM	24.88$\pm$0.16	40.290$\pm$0.14
100 nM	3.166$\pm$0.24	931.00$\pm$0.90
1000 nM	6.168$\pm$0.11	1214.0$\pm$3.0

Table S4. Summary of fitting statistics for real-time ζ-potential measurements of neutravidin-biotin binding. Except for the 10 nM experiment, R-squared values approached unity. In all three cases, the adjusted R-squared value was close to the model R-squared.

Neutravidin Concentration	RMSE	R-squared	Adj. R-squared
10 nM	2.955	0.6722	0.6720
100 nM	29.84	0.9598	0.9597
1000 nM	61.64	0.9135	0.9134

Table S5. Summary of fitting statistics for QCM measurements of neutravidin-biotin binding. Except for the 1000 nM experiment, R-squared values approached unity. In all three cases, the adjusted R-squared value was close to the model R-squared.

Neutravidin Concentration	RMSE	R-squared	Adj. R-squared
10 nM	1.315	0.9078	0.9077
100 nM	1.383	0.8837	0.8836
1000 nM	2.291	0.7416	0.7414

4 Fluorescence measurements of streptavidin binding on biotinylated surfaces

Fluorescence measurements were employed to verify that biotin-streptavidin binding had occurred (Figure S5). We compared the fluorescence intensities of adsorbed streptavidin on three sets of surfaces- PPX-alkyne without clicked biotin, PEG tethered to PPX-alkyne and PPX-alkyne decorated with biotinylated PEG. The first two did not show any fluorescence, indicating that streptavidin did not bind to these surfaces. The biotinylated surface displays a high fluorescence intensity of adsorbed streptavidin, indicating that the binding was specific in nature.

5 Raw ζ-potential data for nanoparticle experiments

The unprocessed ζ-potential values for Figures 4A-C in the paper are furnished without baseline subtraction. This has been plotted in Figure S6 for the six surfaces. Three sets of copolymers with varying isoelectric points (5.7, 4.8 and 3.6) were examined before and after SI-ATRP of sorbitol methacrylate.

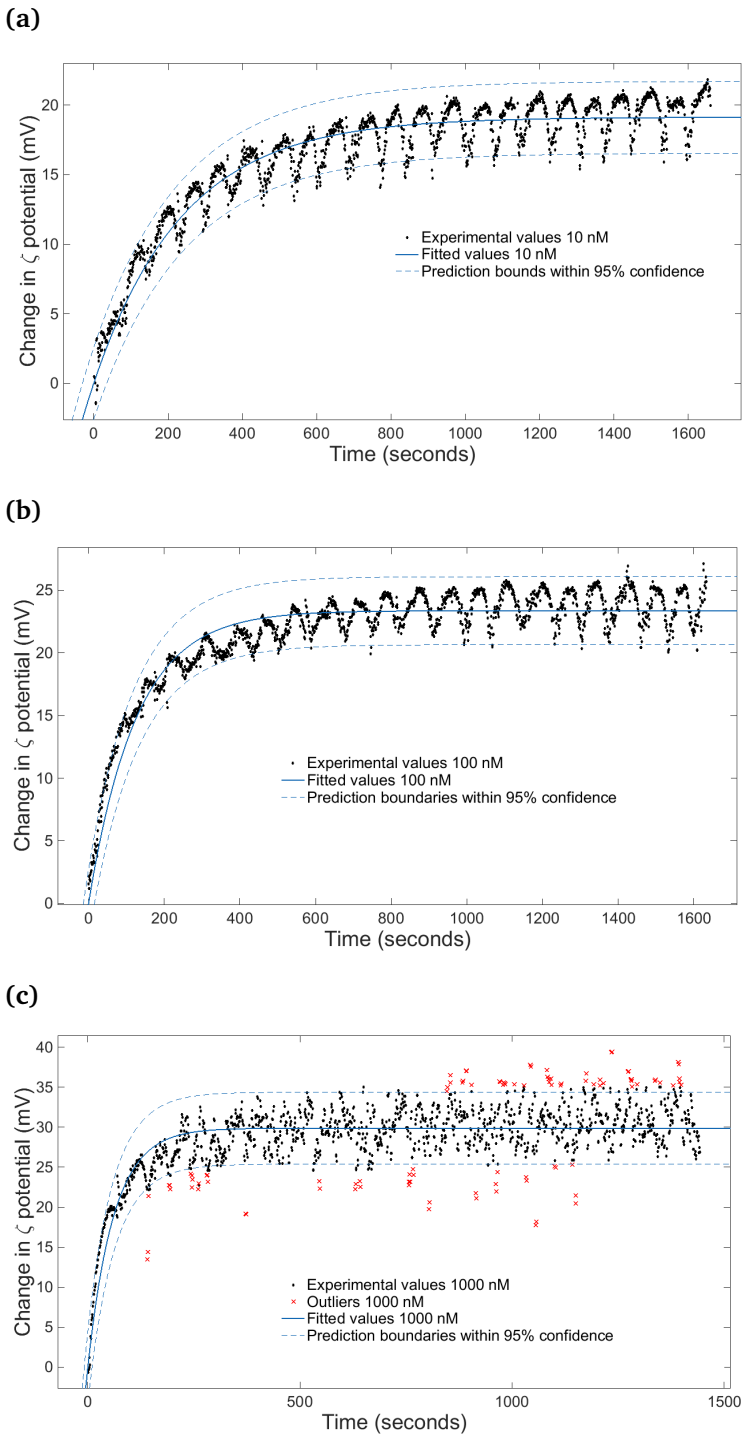

Figure S3. Experimental values from the real-time ζ-potential measurements of A)10 nM, B)100 nM and C) 1000 nM neutravidin on biotinylated surfaces were fitted using a first order equation. The trendline of model values (solid blue line) compares well with experimental values (black dots). Experimental values fall within the prediction boundaries within a 95 % confidence interval. Outliers (indicated in red) were removed from the 1000 nM fit

(a)

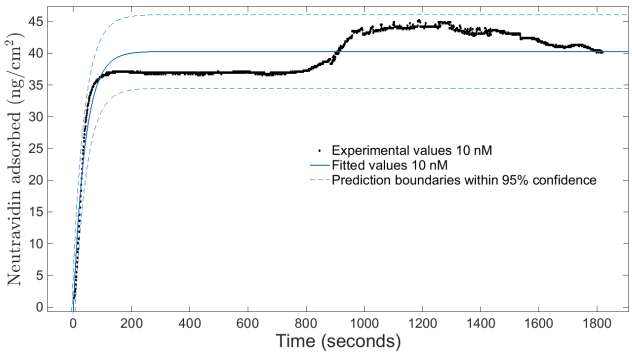

(b)

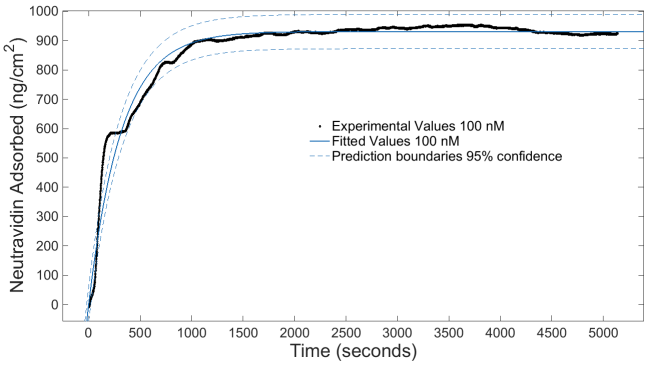

(c)

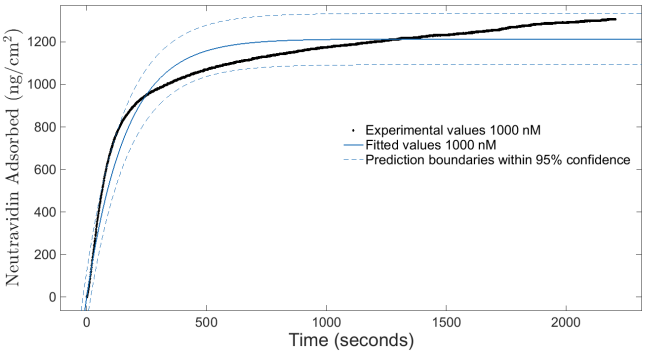

Figure S4. Experimental values from the QCM adsorption measurements of A)10 nM, B)100 nM and C) 1000 nM neutravidin on biotinylated surfaces were fitted using a first order equation. The trendline of model values (solid blue line) compares well with experimental values (black dots). Experimental values fall within the prediction boundaries within a 95 % confidence interval.

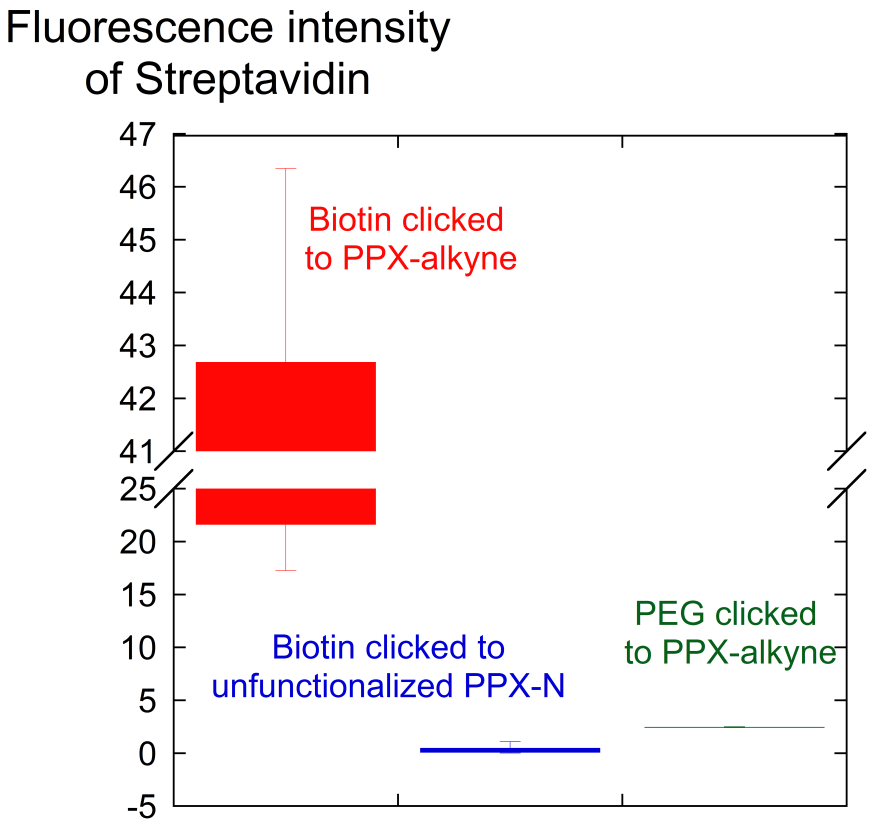

Figure S5. A comparison of fluorescence intensity of streptavidin on biotinylated surfaces with controls indicates that streptavidin adsorption was specific.

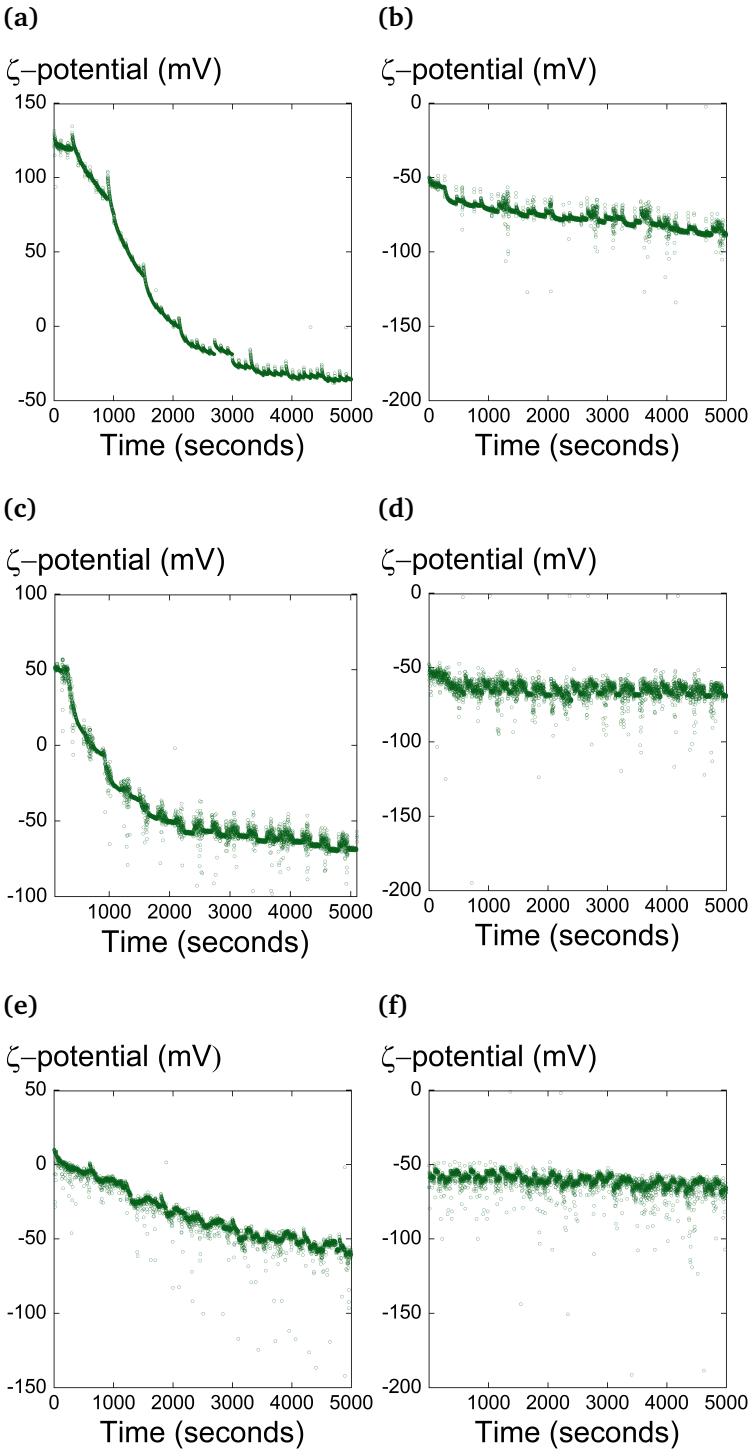

Figure S6. Variation of ζ-potential with time after nanoparticle addition for 3 copolymer surfaces. Copolymer with IEP of 5.7 before (A) and after (B) SI-ATRP of sorbitol. Copolymer with IEP of 4.8 before (C) and after (D) SI-ATRP of sorbitol. Copolymer with IEP of 3.6 before (E) and after (F) SI-ATRP of sorbitol.